



Mangrove Carbon Pool Patterns in Maharashtra, India

Satish N. Pardeshi¹  · Manoj Chavan¹ · Manish Kale¹ · Manoj Khare¹ · Nikhil Lele² · B. K. Bhattacharya²

Received: 5 October 2023 / Accepted: 18 January 2024 / Published online: 2 March 2024
© Indian Society of Remote Sensing 2024

Abstract

This study attempts to investigate whether the mangroves of Maharashtra, India, are acting as a source or sink of carbon. Additionally, efforts were made to develop the empirical model using ground-based tree biomass and satellite-based indices to estimate above-ground biomass (AGB) for the state of Maharashtra for the year 2018–19. Total of 44 geotagged, well-distributed sample plots (0.1 ha each) were laid down to measure the tree girth and height (of all the trees) of different mangrove species. The available biomass equations were used to estimate the AGB at the plot level. Normalized Difference Vegetation Index (NDVI) and plot-wise AGB correlation were tested for minimum, maximum, sum and amplitude of stacked monthly NDVI. The strongest correlation of AGB was observed with maximum NDVI and was therefore used in regression analysis to estimate the AGB and carbon present in mangroves. Carbon values ranged from 2.78 to 249.64 t C ha⁻¹. Carbon sequestration was estimated using statistical method by estimating the difference in total carbon content within the mangroves between the years 2005–06 and 2018–19. Total carbon content was determined by multiplying per hectare AGB with the mangrove area for the respective years. In 2005–06, the carbon pool in the state amounted to 1.08 × 10⁶ tonnes, which increased to 1.32 × 10⁶ tonnes by 2018–19. The mangroves in Maharashtra sequestered a total of 0.24 × 10⁶ tonnes of carbon from 2005–06 to 2018–19, confirming their role as a carbon sink.

Keywords Mangrove · Biomass change · AGB · Carbon · Remote sensing

Introduction

Mangroves are highly productive ecosystems (Alongi, 2015) and are considered the largest potential sinks of atmospheric carbon (Matsui et al., 2010). They are among the most carbon-rich biomes, with an average of 937 t C ha⁻¹ (Alongi, 2015). Many studies conducted worldwide have observed that mangrove forests have significantly higher carbon sequestration rates compared to other forest types (Nyanga, 2020). According to Gibbs et al. (2007), mangroves and their associated environments alone capture more than 55% of biological carbon, often referred as 'green carbon'.

The ongoing debate regarding whether forests act as sources or sinks of carbon dioxide (CO₂) continues to this day (Devi et al., 2023; Harris et al., 2021; Trumper, 2009).

The reason behind this is, on one hand, the forest sequesters atmospheric CO₂, and on the other hand, sequestered CO₂ is lost when the forests are removed. When the carbon sequestration rate is higher than the rate of carbon loss, the forests act as a sink of carbon, whereas when the carbon loss rate is higher than the rate of carbon sequestration, the forests act as carbon source.

The carbon pool can be estimated through the assessment of vegetation biomass. In many studies, it has been noted that carbon typically account for 43% to 50% of the total AGB (Ma et al., 2018). Traditional AGB estimation methods were inherently destructive, involving the felling of trees to assess component-wise AGB after oven drying. Later on methods were developed to estimate bole AGB by non-destructive/least destructive methods which involved extracting small bole sample using a corer, oven drying, and extrapolating the observations to the tree level using different observations, i.e. tree girth and height (Tiwari, 1992; Kale et al., 2015).

The values estimated using these methods provide the primary data for AGB estimation. Nevertheless, developing species and area-specific biomass equations, even

✉ Satish N. Pardeshi
satishp@cdac.in; satishpardeshi@gmail.com

¹ Centre for Development of Advanced Computing (C-DAC), Pune, India

² Space Application Centre, Indian Space Research Organization (ISRO), Ahmedabad, India

with non-destructive approaches, poses a challenge. This challenge arises from the need for a large number of bole samples across various girth classes, representing diverse climatic, edaphic, and topographical conditions. Due to these reasons, there is a dearth of species and area-specific biomass equations particularly for mangrove species in the Indian context. The Forest Survey of India (FSI) has undertaken significant efforts to formulate tree volume equations for different tree species in the country (Brahma, et al., 2021; FSI., 1996). Such volume equations have been utilized for AGB estimation in numerous studies (Kale et al., 2009; Saxena et al., 2003); however, for many tree species, these equations are still lacking.

Satellite remote sensing plays a crucial role in mapping mangrove ecosystems, primarily because traversing through mangroves for field-based investigations is challenging due to harsh environment. The synoptic view provided by the remote sensors helps in regular monitoring of mangroves (Blasco et al., 2001; Kumar et al., 2013). Wang et al. (2019) conducted a comprehensive review of remote sensing of mangroves from 1956 to 2018, emphasizing its role in mapping, estimating biophysical parameters, and characterizing ecosystem processes within mangroves.

While most of the earlier studies primarily focused on mapping the extent of mangroves, recent research, particularly from 2012 onwards, has shifted its emphasis towards climate change (Mandal & Bar, 2018), Leaf Area Index (LAI) (Gnanamoorthy et al., 2021), carbon flux (Zhao et al., 2022), Light Use Efficiency (LUE) (Lele et al., 2021), and evapo-transpiration (Zhu et al., 2020) estimations. Numerous satellite datasets, including Landsat since 1972 (Goward et al., 2006), SPOT since 1985 (Chevrel et al., 1981), IKONOS since 1999 (Dial et al., 2003), MODIS since 2000 (Justice et al., 2002), Quick Bird since 2001 (Toutin et al., 2002), World View since 2007 (Poli et al., 2009), Gaofen since 2013 (Chen et al., 2022), and Sentinel since 2015 (Nagler et al., 2015), have been utilized in various studies related to mangrove mapping, biophysical parameter estimation, and climate change research (Wang, 2019).

With the availability of free satellite datasets such as Sentinel 2 having 10 m resolution and a revisit time of 5 days, high-resolution temporal and spatial mapping of mangroves has become more feasible. Moreover, Sentinel 2 data have been found to be more accurate in predicting AGB using vegetation indices than that of Landsat 8 (Nguyen & Nguyen, 2021). Additionally, satellite data from LISS IV, which includes visible and, near-infrared (NIR) with a spatial resolution of 5.8 m, have been proved extremely valuable in carrying out mangrove community zonation mapping. Furthermore, the synthesized LISS IV band (Rout et al., 2019) has been found highly effective in distinguishing between mangrove and non-mangrove vegetation. Precise mangrove classification is crucial to ensure

the accurate estimation of carbon stocks. Satellite remote sensing has been extensively used in developing empirical biomass models for pixel level biomass estimation. Different satellite-derived indices such as Normalized Difference Vegetation Index (NDVI), Ratio vegetation index (RVI), and Enhanced vegetation index (EVI) have been found highly correlated with ground-based AGB observations (Li et al., 2007; Alatorre et al., 2012) and improves the estimation accuracy (Opelele et al., 2021; Singh et al., 2023; Sun et al., 2015), thus can be effectively used in regional level AGB estimation using empirical models.

Carbon budget studies are important because of their linkage with changing climate. Mangrove can be part of the REDD + mechanism to bring additional financial resources to the mangroves and develop comprehensive management and conservation activities (Ajonina et al., 2014). Such goals can be achieved based on the robust and accurate carbon budget studies.

The present research is aimed at the estimation of carbon pools of mangroves of Maharashtra, developing an empirical model for ha^{-1} AGB estimation and studying the carbon pool for 2005–06 and 2018–19, to understand whether the mangroves of Maharashtra are source or sink of carbon.

Study Area

The study was carried out in the mangrove vegetation of Maharashtra, which lies along the west coast of India between $15^{\circ} 45'$ to $20^{\circ} 00'$ N latitudes and $68^{\circ} 00'$ to $73^{\circ} 30'$ E longitudes having a coast line of 720 km. (Ajai et al., 2012) (Fig. 1).

The shoreline is oriented more or less north–south, bounded by the Arabian Sea in the west and the Western Ghats in the east. The coastal track is relatively broader in the north and narrows down in the south and is characterized by pocket beaches flanked by rocky cliffs of Deccan basalt. Highly dissected coastal topography forms the principal governing feature along southern Maharashtra coastal districts with numerous faults (Ajai et al., 2012). About 70% of the coast has patches of mangrove vegetation spreading inwards around 44 creeks (Gnanappazham, 2020). There are about 34 pocket beaches along the coast line (Gunasekaran et al., 2022). The shoreline stretches from Zai Creek bordering Gujarat in the North to the Terekhol River bordering Goa in the South. All the six coastal districts have coastal/riverine mangrove vegetation, spread across 35 talukas with Raigarh district having maximum mangrove vegetation (41.64%) followed by Mumbai (15.49%), Thane (14.73%), Palghar (13.53%), Ratnagiri (10.21%) and Sindhudurg district (4.4%) as on 2018–19. The dominant mangrove species

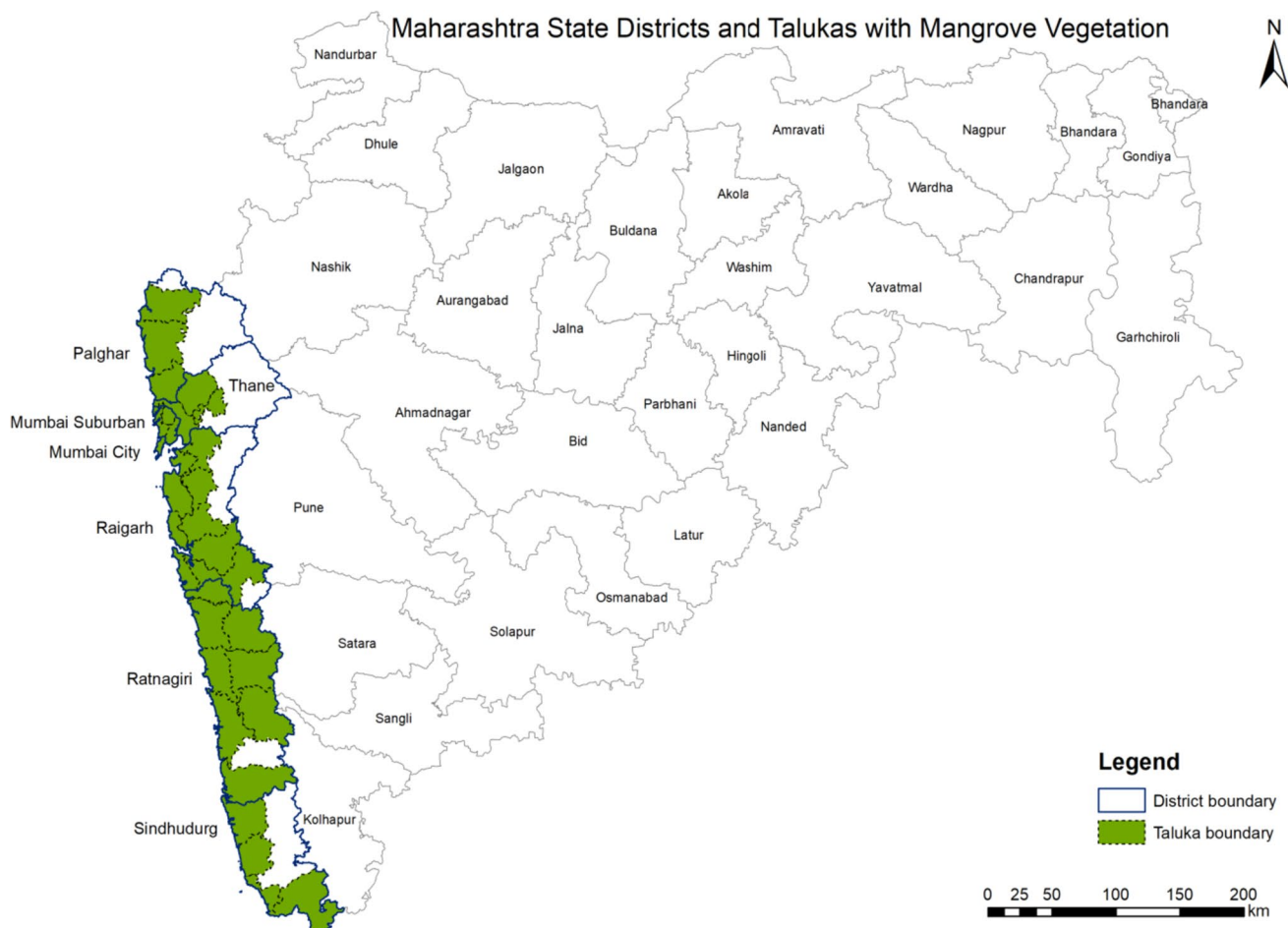


Fig. 1 Maharashtra state- districts and taluka map having mangrove vegetation (source-District boundary, Survey of India, 2023)

being *Avicennia marina* (Forssk.) Vierh., *Sonneratia alba* J. Smith, and *Avicennia officinalis* L.

Materials and Method

Indian Remote Sensing satellite (IRS)—Linear Imaging Self Scanning Sensors (LISS) IV (low-tide) data (including the LISS IV SWIR synthetic band) for the year 2018–19 and IRS—LISS III data of 2005–06 were used for mangrove extent mapping and carbon sequestration estimation. Atmospherically corrected Sentinel 2 data (2018–19) with a spatial resolution of 10 m were used for spectral response modelling and developing an empirical model for per pixel biomass estimation.

Mangrove Mapping

The IRS P6 LISS IV low tide satellite images were used for mapping mangrove class (dense and Open) using the on-screen digitization method at 1:25,000 scale, based on

the basic elements of visual interpretation like tone, texture, shape, size and association. The synthetic IRS LISS IV SWIR data were used mainly to separate out the mangrove and non-mangrove vegetation. The SACRS2 (Scheme for Atmospheric Correction of Resourcesat-2 (RS2) AWiFS data) package developed by Space Application Centre, ISRO was used for processing LISS IV data and converting digital numbers to reflectance before merging SWIR band (Pandya et al., 2014, Rout et al., 2019).

A total of 20 mangrove species and 95 mangrove associates were encountered in the study area (supplementary material (1)). These mangrove species in different association were delineated into 32 mangrove communities. The reference of field-based investigations and Google Earth images (Google, 2022) was taken to delineate the communities. These communities were homogenized to prepare the mangrove extent map covering dense and open mangrove categories for the year 2018–19. This map was overlaid on the cloud free IRS LISS III satellite data of the year 2005–06 to delineate the change in mangrove extents in accordance with the methodology adopted by Roy et al.

(2016) and Meiyappan et al. (2017). For all the interpretations, low-tide LISS III satellite data were used, however, wherever low tide data were not available, historical available Google Earth low tide images were referred for confirming the mangrove extents. The tidal status of satellite data used were confirmed using the historical tide timings using the application available at <https://tides4fishing.com/lunar-calendar> app.

The variations in the tide have a significant effect on mangrove delineation, as the mangrove gets completely or partially inundated during high tide, the spectral signatures of mangroves get altered (Xia et al., 2018). This also affects the interpretation of mangrove spatial extent, thereby influencing the estimation of mangrove area (Supplementary material 2.jpeg).

In addition to this, Landsat-8 OLI (30 m) imageries for the year 2018–19 were also used for validation purpose. Multi-date high-resolution Google Earth Pro imageries were referred for confirmation of doubtful areas, and demarcation of closely associated classes like orchards and salt marsh.

Field Investigations

Field investigations were carried out for ground truthing and laying random fixed sample plots (0.1 ha) for making observations related to tree AGB estimation between October 2019—October 2022. Total 0.01% sampling of the total mangrove area (376 km²) was carried out which required a minimum of 38 plots. In the present study, a total of 44 sample plots were laid down (Fig. 2).

Parameters like image tone and texture variability, distance from the coast, salinity status, fresh water availability and geomorphology were considered to lay down the ground sample plots. Plots were planned in such a way that maximum tonal variability owing to different species and their associations were addressed. Attempts were made to lay the sample plot during the low tide. Once the desired location was reached, the centre tree was marked (C1) with the metal plate attached to a loose string. Corner trees of the plot were marked as C2, C3, C4 and C5, respectively (Supplementary material 3.jpeg). A detailed inventory of all the identified mangrove trees, shrubs and herbs was carried out. In case of doubtful identity, species photographs were taken to carry out identification in laboratory.

All the trees falling inside the plots were identified to the species level and measured for their height (m) and CBH (circumference at breast height (cm)). The visual evidence of disturbance, i.e. lopping/grazing/fire, was recorded. The vegetation type as observed on the field was also recorded.

The preliminary mangrove map prepared was validated on the ground for different mangrove classes and necessary

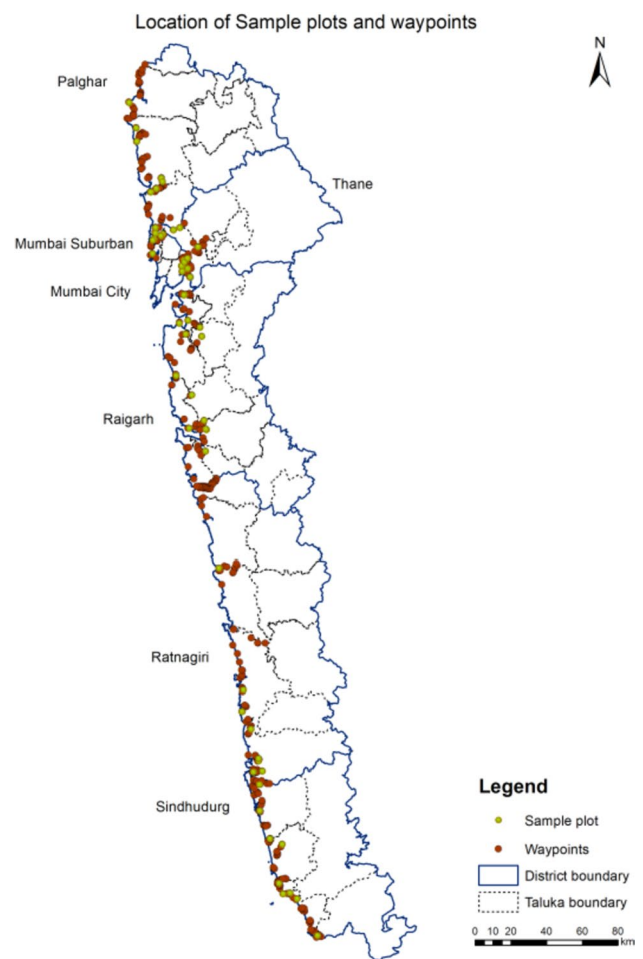


Fig. 2 Sample plots and waypoints distribution

corrections were made. Total 500+ way points throughout the mangrove areas were collected, and their attributes were recorded. These were used for post-field validation of the mangrove (open and dense class) and non-mangrove classes (Fig. 2).

Biomass and Carbon Pool Estimation

The tree AGB was estimated using the available allometric equations available in the literature (Table 1).

The plot-wise AGB provides the biomass for 0.1 ha which was averaged to ha⁻¹ AGB separately for dense and open mangroves. The carbon stock was estimated using the equation $C_{ag} = 0.50 W_{ag}$ (where C_{ag} is the above-ground carbon stock, and W_{ag} is the AGB) (Brown, 1997; Petersson et al., 2012).

For the present study, whenever possible, species-specific equations were utilized from the literature, taking into account the unique characteristics and attributes of individual mangrove species, however, in cases where,

Table 1 The Allometric equations used for estimation of AGB

No	Allometric equation (above-ground biomass)	Species	Reference
1	$0.1848D^{2.3524}$	<i>Avicennia marina</i> (Forssk.) Vierh	Dharmawan and Siregar (2008)
2	$0.1466D^{2.3136}$	<i>Rhizophora mucronata</i> Lam	Dharmawan and Siregar (2008)
3	$0.0275 D^{3.22}$	<i>Rhizophora apiculata</i> Bl	Pambudi (2011)
4	$0.251pD^{2.46}$	<i>Avicennia officinalis</i> L	Komiyama (2005)
5	$0.168pD^{2.47}$	<i>Aegiceras corniculatum</i> (L.) Blanco	Chave et al. (2005)
6	$0.251pD^{2.46}$	<i>Bruguiera cylindrica</i> (L.) Blume	Komiyama (2005)
7	$0.168pD^{2.47}$	<i>Excoecaria agallocha</i> L	Chave et al. (2005)
8	$0.168pD^{2.47}$	<i>Heritiera littoralis</i> Dryand. ex Aiton	Chave et al. (2005)
9	$0.163D^{2.37}$	<i>Lumnitzera racemosa</i> Willd	Nam (2009)
10	$0.105D^{2.68}$	<i>R. mucronata</i> Lam	Zanne et al. (2009)
11	$0.0825*(D^2H)^{0.89966*p}$	<i>Sonneratia alba</i> J. Smith	Kauffman et al. (2011)
12	$0.280(D^2H)^{0.693}$	<i>Sonneratia apetala</i> Buch.-Ham	Wang et al (2015)
13	$0.0341D^{1.03}$	<i>Kandelia candel</i> (Perr.) C.B.Rob	Wang et al (2015)

D – Diameter at breast height (cm); H-maximum height of measured tree (feet), p – wood density (cm^{-3}); *Avicennia officinalis* L. ($p=0.59 \text{ gcm}^{-3}$), *Aegiceras corniculatum* (L.) Blanco ($p=0.51 \text{ gcm}^{-3}$), *Bruguiera cylindrica* (L.) Blume ($p=0.72 \text{ gcm}^{-3}$), *Excoecaria agallocha* L. ($p=0.39 \text{ gcm}^{-3}$), *Heritiera littoralis* Dryand. ex Aiton ($p=0.79 \text{ gcm}^{-3}$), *Sonneratia alba* J. Smith ($p=0.078 \text{ gcm}^{-3}$) (Chave et al. 2005)

species-specific equations were not available, generalized equations available were used for the estimation of carbon stocks across diverse mangrove species. The wood density of different mangrove species was obtained from the World Agro Forestry Database (Chave et al., 2009). Since understory vegetation (seedlings and herbs) is negligible in mangrove systems, they were not considered for ecosystem carbon stock estimations (Kauffman and Donato 2011; Harishma et al., 2020).

Biomass Modelling

Out of a total of 44 plots, 36 plots were used for developing the empirical model. The per pixel AGB was estimated using the spectral response modelling approach by experimenting the relationship between plot-wise AGB and different NDVI variants. The Google Earth Engine (GEE) (Gorelick, et al., 2017) was used for obtaining monthly atmospherically corrected NDVI values for the months of October, November, December, January, February, March, April and May (2018–2019) (by applying sensor independent atmospheric correction algorithm (SIAC)) for Sentinel 2A dataset available in the Google Earth Engine archives). The bands used to calculate NDVI indices were B4 (red) and B8 (NIR). Only dataset having less than 10% cloud percentage were used. Whenever more than one satellite data were available for each month, the date in which the maximum value of the NDVI was available was used for monthly stacking. Different NDVI variants, i.e. maximum, minimum, sum and amplitude NDVIs, were obtained from the stacked NDVIs of October 2018 to May 2019. Maximum NDVI is the maximum NDVI value obtained from all the months considered

together, whereas, minimum and sum NDVI are minimum and aggregated NDVI values respectively obtained from all the months considered together. The amplitude NDVI is the difference between the minimum and maximum NDVI values obtained when all the months were considered together. All the NDVIs were resampled to 30 m x 30 m pixel size to have an exact match with the ground-based plot dimension (Fig. 3).

The plot-wise AGB values were regressed against the different NDVI estimates. The linear, power and exponential models were explored to develop the empirical model. The best model was used to estimate per pixel AGB using the relevant regression equation.

Carbon Sequestration Estimation

The per hectare average carbon present in dense and open mangrove obtained by averaging plot-wise carbon ha^{-1} was extrapolated in the respective classes for the years 2005–06 and 2018–19 to obtained carbon for the year 2005–06 and 2018–19 respectively (Nguyen et al., 2019; Nguyen & Nguyen, 2021). The class-wise difference between carbon amounts for the duration provided class-wise carbon sequestration by mangroves. Based on this, it was determined whether the mangroves of Maharashtra are acting as a source or sink of carbon.

The overall methodology is presented in Fig. 3

In order to make additional validation of the carbon sequestration, MODIS Gross Primary Productivity (MODIS-GPP) product was used. The GPP products for all land areas are available since year 2001 (<https://earthexplor>

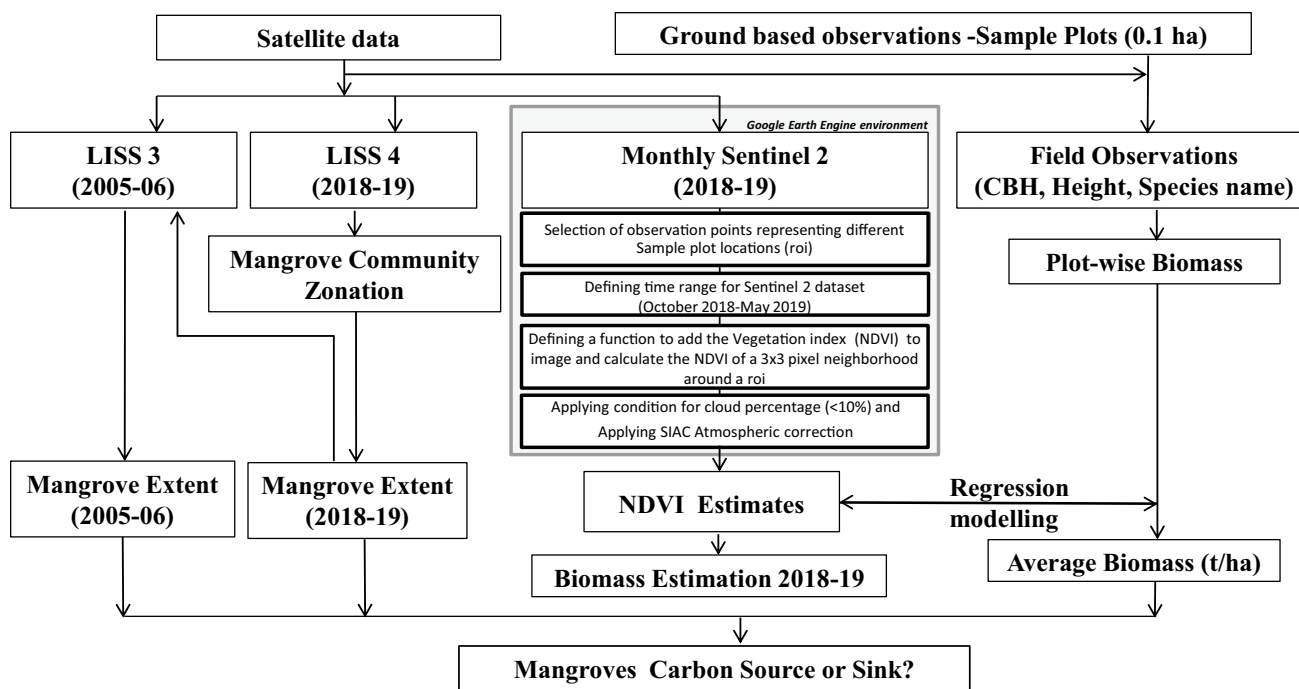


Fig. 3 Approach for AGB estimation

rer.usgs.gov). The products were accessed using Google Earth Engine and annual GPP sum was computed for year 2005–06 and 2018–19. The annual sum for the mangrove area was evaluated using the respective mangrove mask for the year 2005–06 and 2018–19.

Results and Discussion

Mangrove Mapping and Carbon Sequestration

The interpretation of derived map revealed that total mangrove area in the Maharashtra state in the year 2018–19 was 376.13 km². Total mangrove area under dense (density > 40%) and open mangroves (density < 10–40%) forests in the year 2018–19 was 210.50 km² and 165.71 km², respectively (Fig. 4a and b). In Maharashtra the dominant mangrove species is *Avicennia marina* (Forssk.) Vierh., followed by *Sonneratia alba* J. Smith and *Rhizophora mucronata* Lam. The dominant mangrove species in northern Maharashtra is *Avicennia marina* (Forssk.) Vierh. (78%), followed by *Sonneratia apetala* Buch.-Ham. (11%) and *Sonneratia alba* J. Smith. (7%), whereas, the dominant species in southern Maharashtra is *Avicennia officinalis* L. (31%) followed by *Sonneratia alba* J. Smith (27%) and *Rhizophora mucronata* Lam (17%) (Supplementary material 1.doc).

From 2005–06 to 2018–19, there was an increase of 71.75 km² of mangrove area. The dense mangrove increased from

176.77 km² in 2005–06 to 210.50 km² in 2018–19. The open mangrove increased from 127.69 km² in 2005–06 to 165.71 km² in 2018–19. The open mangrove transformed to dense mangrove is 37.84 km², whereas, the dense mangrove converted to open mangrove is 23.31 km². New areas that came under mangrove cover were 93.65 km² out of which open mangrove is 66.56 km² and dense mangrove is 27.26 km². Total area lost to natural and anthropogenic factors was 22.02 km² out of which 13.96 km² were open and 8.06 km² were dense mangroves. The primary causes for the loss of mangrove are developmental activities, aquaculture, reclamation, habitat loss and erosion, whereas, an increase in mangrove area is attributed to siltation (Mendiratta et al., 2015) and sea water inundation of cropland areas as it formed new grounds for the establishment of the mangroves. Along with this plantation and protection by the forest department also contributed to an increase in mangrove area.

The total carbon sequestered by the mangroves from the year 2005–05 to 2018–19 is 0.24×10^6 tonnes, out of these open mangroves sequestered 0.10×10^6 tonnes of carbon, whereas, dense mangroves sequestered 0.15×10^6 tonnes of carbon (Table 2). It is therefore the mangroves are found to be the net sink of carbon.

The value of carbon estimated in the present study is in accordance with similar studies carried out in the mangrove forest. In recent studies Ragavan et al. (2021), reported an average vegetation carbon stock of $290.26 \pm 319.96 \pm 27.28$ t C ha⁻¹ for the Andaman region. Rani et al. (2023) reported carbon from Kochi with a range

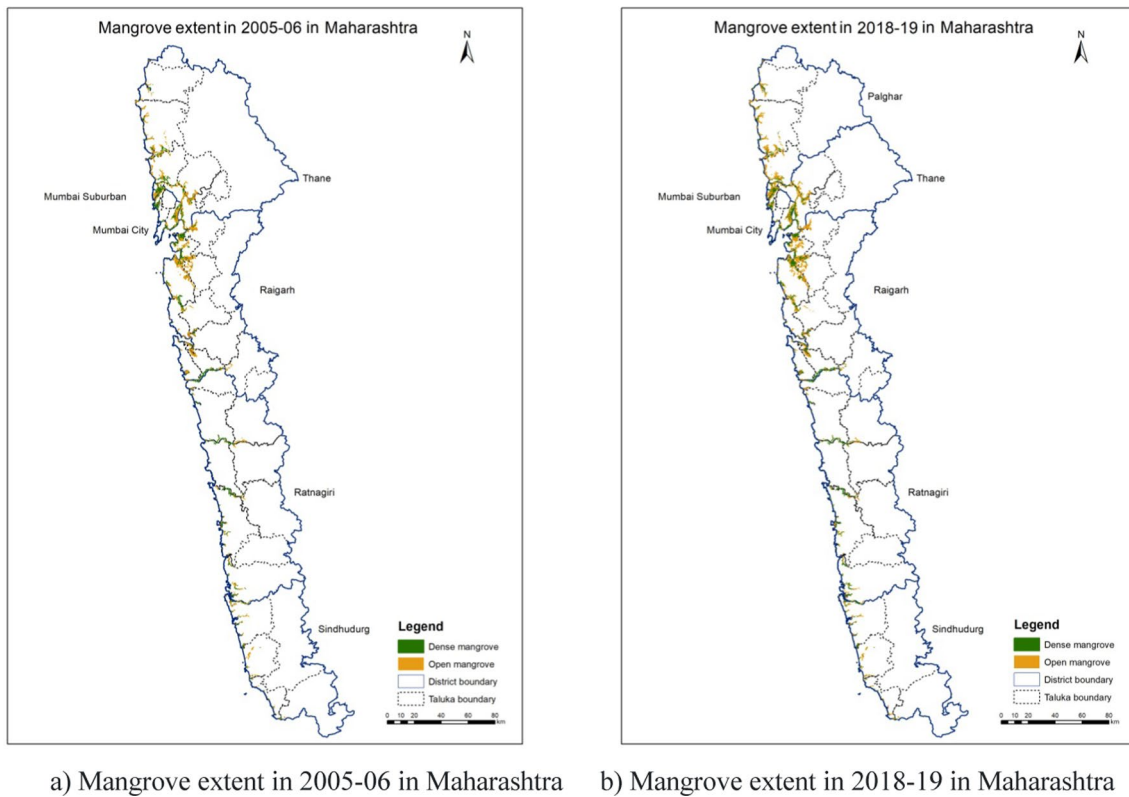


Fig. 4 a Mangrove extent in 2005–06 in Maharashtra. b Mangrove extent in 2018–19 in Maharashtra

Table 2 Carbon sequestration patterns in the mangroves of Maharashtra

	Year 2005–06	Year 2018–19	Difference
Carbon in open mangrove (25.14 ha ⁻¹)	0.32 × 10 ⁶	0.42 × 10 ⁶	0.10 × 10 ⁶
Carbon in dense mangrove 43.07 ha ⁻¹)	0.76 × 10 ⁶	0.91 × 10 ⁶	0.15 × 10 ⁶
Total carbon (tonnes)	1.08 × 10 ⁶	1.32 × 10 ⁶	0.24 × 10 ⁶

of AGB of $171.68 \pm 104.42 \text{ t C ha}^{-1}$ and Banerjee et al. (2021) reported total carbon (TC) in a range of 51.35 ± 6.77 to $322.47 \pm 110.79 \text{ t C ha}^{-1}$ from Bhitarkanika Wildlife Sanctuary, which is in an acceptable range of the currently estimated carbon study.

The carbon pools of AGB estimated by Kauffman et al. (2011) in the Micronesian mangrove forests was $104.4 \text{ t C ha}^{-1}$ at Palau and $169.2 \text{ t C ha}^{-1}$ at Yap. whereas, Donato et al. (2011) estimated an average $1127.664 \text{ t C ha}^{-1}$ in Indo-pacific region mangroves. These were much higher than the above-ground carbon pools estimated in the present study (highest carbon of $249.69 \text{ t C ha}^{-1}$). Majority of these mangroves forests (like Andaman, Bhitarkanika, Kochi, etc.,) are quite different and dense compared to mangrove cover of Maharashtra. It is important to note that some sites in Northern Maharashtra are dense but short-heighted (1–3 feet) *Avicennia marina* (Forssk.)

Vierh that covers a sizable area on the ground and may have an effect on overall AGB values of the region.

The AGB increase was corroborated using MODIS-GPP product. Annual sum of GPP for the mangrove area for the year 2006 was found to be 558,880 t C, while in 2018 it was 688,170 t C. The difference in GPP thus indicated an increase in mangrove productivity between 2006 and 2018 by 129,290 t C. The GPP increase is possible by the increase in mangrove area and also an increase in carbon sequestration by existing mangroves. Overall, an increase in GPP and an increase in AGB of mangroves suggest that the mangroves of Maharashtra are functioning as carbon sink.

Biomass Modelling

The attempts were made to establish the correlation between plot-wise AGB and NDVI. Out of the different NDVI variants experimented, the maximum NDVI exhibited the best relationship with plot-wise AGB (Fig. 5). On examining the scatter plot it was observed that the biomass was well correlated with maximum NDVI, when the power model was used. The R^2 obtained for the power model was highest ($R^2=0.43$) among all studied model for maximum NDVI. The AGB-maximum NDVI correlation pattern analysis and R^2 values were considered for finalizing the model.

The plots located in the close proximity of non-mangrove areas were avoided for the development of the empirical model. The equation used for regional level AGB estimation was of the form:

$$Y = 350574x^{8.5344}$$

where Y = biomass in kg, and x is maximum NDVI.

This relationship was used to extrapolate the AGB values to the complete study area.

The performance of empirical models developed using different NDVI variants is listed in Table 3. The maximum NDVI (which depicted a higher correlation with AGB) represents the full grown status of mangroves post-monsoon. Thus, the maximum NDVI can be used as a proxy to

Table 3 The empirical models experimented

NDVI variant	Empirical model	R^2 (Coefficient of determination)
Maximum NDVI	Linear	$R^2=0.27$
	Exponential	$R^2=0.40$
	Power	$R^2=0.43$
Minimum NDVI	Linear	$R^2=0.21$
	Exponential	$R^2=0.30$
	Power	$R^2=0.40$
Amplitude NDVI	Linear	$R^2=0.01$
	Exponential	$R^2=0.001$
	Power	$R^2=0.0003$
Sum NDVI	Linear	$R^2=0.003$
	Exponential	$R^2=0.019$
	Power	$R^2=0.007$

Biomass modelling

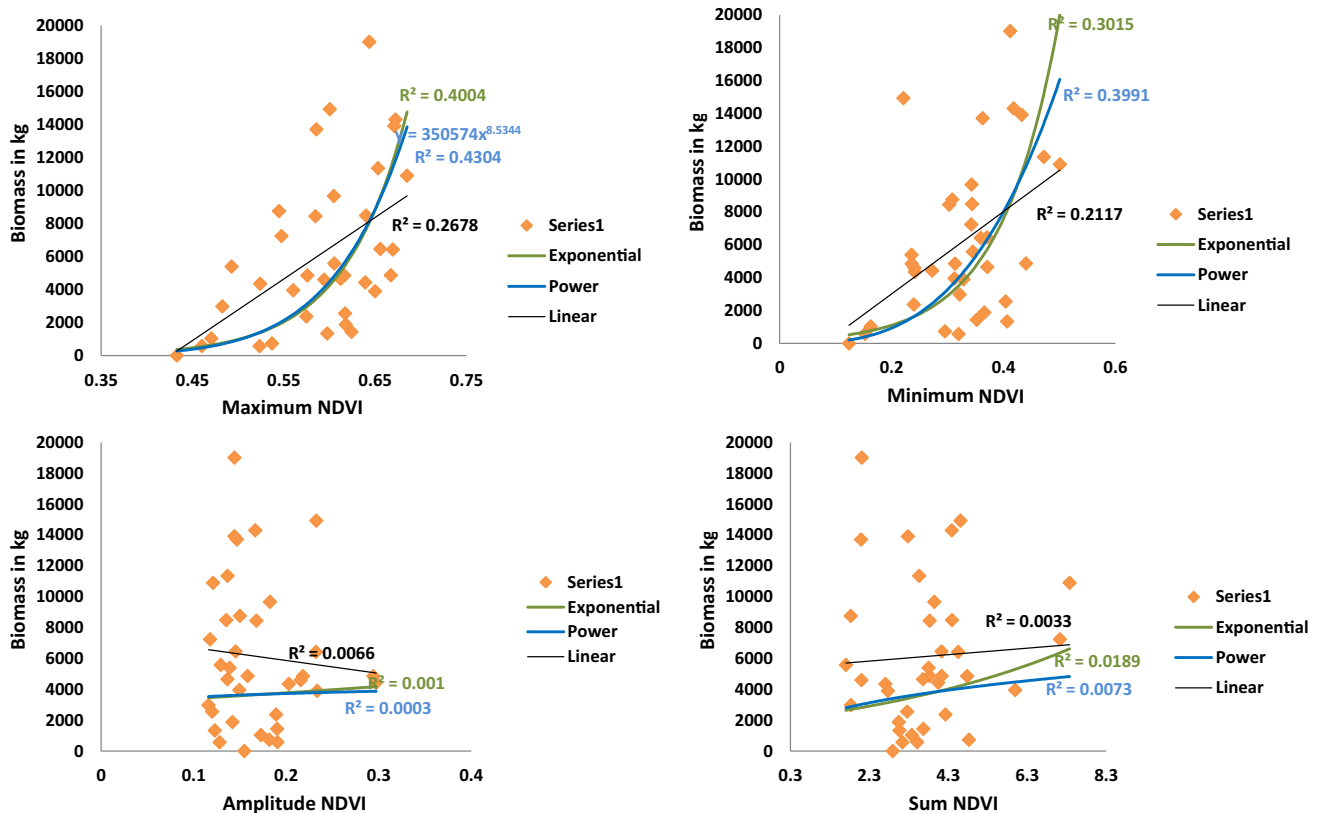


Fig. 5 Correlation of biomass with NDVI variants

investigate the canopy changes (and therefore the biomass) at different locations, at different periods of time.

Carbon in the mangroves of Maharashtra for the year 2018–19 varied between 2.78 and 249.64 tonnes (Fig. 6). Mangroves of southern Maharashtra stored a higher amount of carbon compared to mangroves of northern Maharashtra. This is attributed to a higher level of disturbance in the mangroves of northern Maharashtra as compared to mangroves of southern Maharashtra. High amount of carbon was observed in the areas of Achra, Vaghotan, Dorle and Sagave villages, whereas, comparatively less amount of carbon was observed in the areas around Thane creek, Mhasala and Nhava-Sheva, Pen. In general, the island mangroves have a higher amount of carbon in both northern and southern Maharashtra as less anthropogenic disturbance has been observed in these regions.

Conclusion

The study explores the utility of LISS-IV data for mangrove community zonation, use of NDVI variants for estimation of mangrove AGB and study the patterns of mangrove above-ground carbon pools in Maharashtra. Amongst all variants, maximum NDVI has been found most suitable for estimation of AGB using satellite data.

Carbon pool in mangroves in the state depicts a clear pattern that mangroves in the southern Maharashtra store a higher amount of carbon compared to mangroves of the northern part of the state. This is also evident from the fact that there are diverse and dense patches of mangroves in the southern region compared to northern Maharashtra. The highest (more than 20 t C ha^{-1}) amount of carbon in the mangroves was found at Ganpatipule, Jaigad, Guhagar, Dapoli Taluka at Ratnagiri district, areas along Muchkundi

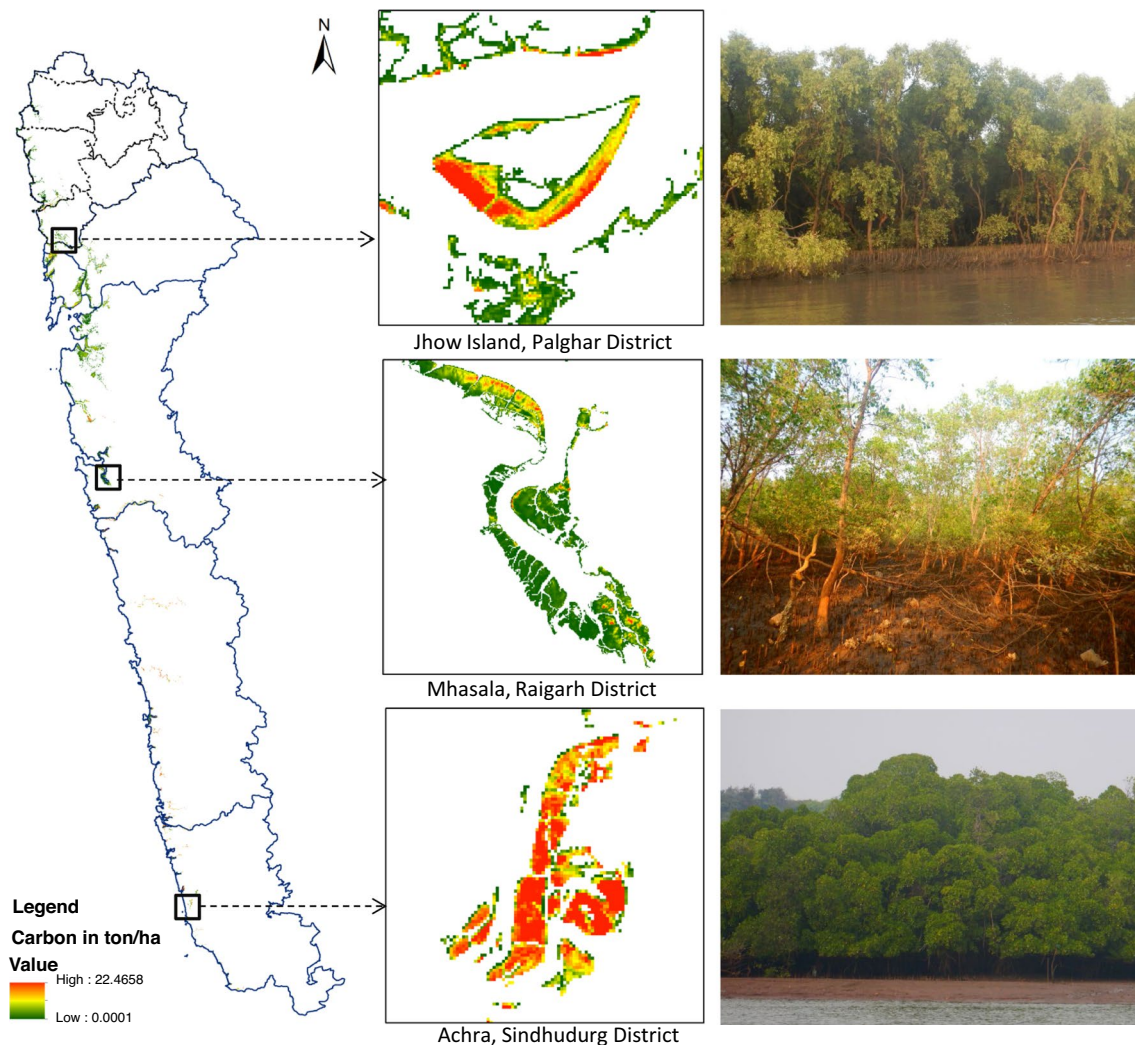


Fig. 6 Carbon map derived using maximum NDVI empirical model of Maharashtra for year 2018–19

and Vashisthi river in Ratnagiri district and at Kudal Taluka in Sindhudurg district of the state. The study highlights an increase in overall mangrove cover of the state and an associated rise in carbon sequestration, suggesting that the mangroves in Maharashtra are serving as potential carbon sink.

The per ha carbon map generated in the present study will help administrators and policy makers to formulate policies and prioritize areas for the management and protection of mangroves.

Mangroves of Maharashtra are playing an important role in harvesting the atmospheric carbon and abatement of climate change. It is therefore, they can effectively contribute in United Nation's sustainable goal no. 13 (Climate Action). With effective afforestation the sinks can further be increased. Several studies have highlighted that mangroves sequester high amount of carbon dioxide and it is therefore, important to carry out further research on the development of the species and area-specific AGB equations for the mangroves found along the Western Ghats of India. This will ensure high accuracy carbon budgeting of mangrove ecosystems of the Arabian Sea.

Supplementary Information The online version contains supplementary material available at <https://doi.org/10.1007/s12524-024-01823-3>.

Acknowledgements The present paper is outcome of the project funded by Space Application Centre, Indian Space Research Organisation (ISRO). Mangrove Cell, Government of Maharashtra is acknowledged for providing necessary permissions and ground support throughout the project duration.

Author Contribution All authors contributed to the study conception and design. Material preparation, data collection and analysis were performed by Satish N Pardeshi, Manoj Chavan, Manish Kale and Nikhil Lele. Guidance on methodology and interpretation was provided by B.K. Bhattacharya. The first draft of the manuscript was written by Satish N Pardeshi and Manish Kale, and all authors commented on previous versions of the manuscript. All authors read and approved the final manuscript.

Funding The project was carried out from active funding from Space Application Centre, Indian Space Research Organisation (ISRO), Ahmedabad, India.

Declarations

Conflict of interest The authors declared that they have no conflict of interest.

References

- Ajai, N.S., Tamilarasan, V., Chauhan, H.B., Bahuguna, A., Gupta, C., Rajawat, A.S., Chaudhury, N.R., Kumar, T., Rao, R.S., Bhattacharya, S. & Ramakrishnan, R. (2012). Coastal zones of India. *Ahmedabad: Space Applications Centre, (ISRO)*. <https://doi.org/10.1080/10095020.2017.1333715>
- Ajonina, G., Kairo, J.G., Grimsditch, G., Sembres, T., Chuyong, G., Mibog, D. E., Nyambane, A. & FitzGerald, C. (2014). Carbon pools and multiple benefits of mangroves in Central Africa: Assessment for REDD+. 72pp. United Nations Environment Program.
- Alatorre, L. C., Carrillos, S. S., Beltran, S. M., Medina, R. J., Olave, M. E. T., Bravo, L. C., Weibe, L. C., Grandos, A., & Alongi, D. M. (2012). Carbon sequestration in mangrove forests. *Carbon Management*, 3(3), 313–322. <https://doi.org/10.4155/cmt.12.20>
- Alongi, D. M., & Mukhopadhyay, S. K. (2015). Contribution of mangroves to coastal carbon cycling in low latitude seas. *Agricultural and Forest Meteorology*, 213, 266–272. <https://doi.org/10.1016/j.agrformet.2014.10.005>.
- Banerjee, K., Mitra, A., & Villasante, S. (2021). Carbon cycling in mangrove ecosystem of Western Bay of Bengal (India). *Sustainability*, 13(12), 6740. <https://doi.org/10.3390/su13126740>.
- Bijayalaxmi Devi, N., & Lepcha, N. T. (2023). Carbon sink and source function of Eastern Himalayan forests: Implications of change in climate and biotic variables. *Environmental Monitoring and Assessment*. <https://doi.org/10.1007/s10661-023-11460-x>
- Blasco, F., Aizpuru, M., & Gers, C. (2001). Depletion of the mangroves of continental Asia. *Wetl. Ecol. Maag.*, 9, 255–266. <https://doi.org/10.1023/A:1011169025815>.
- Brahma, B., Nath, A. J., Deb, C., Sileshi, G. W., Sahoo, U. K., & Das, A. K. (2021). A critical review of forest biomass estimation equations in India. *Trees, Forests and People*, 5, 100098. <https://doi.org/10.1016/j.tfp.2021.100098>.
- Brown, S. (1997). Estimating biomass and biomass change of tropical forests: A primer. *FAO- Food and Agriculture Organization of the United Nations*, 134, 3–6.
- Chave, J., Andalo, C., Brown, S., Cairns, M. A., Chambers, J. Q., Eamus, D., Fölster, H., Fromard, F., Higuchi, N., Kira, T., Lescuré, J. P., Nelson, B. W., Ogawa, H., Puig, H., Riera, B., & Yamakura, T. (2005). Tree allometry and improved estimation of carbon stocks and balance in tropical forests. *Oecologia*, 145, 87–99. <https://doi.org/10.1007/s00442-005-0100-x>
- Chave, J., Coomes, D., Jansen, S., Lewis, S. L., Swenson, N. G., & Zanne, A. E. (2009). Towards a worldwide wood economics spectrum. *Ecology letters*, 12(4), 351–366. <https://doi.org/10.1111/j.1461-0248.2009.01285.x>.
- Chen, L., Letu, H., Fan, M., Shang, H., Tao, J., Wu, L., & Zhang, T. (2022). An introduction to the Chinese high-resolution Earth observation system: Gaofen-1~7 civilian satellites. *Journal of Remote Sensing*. <https://doi.org/10.34133/2022/9769536>.
- Chevrel, M., Courtois, M. I. C. H. E. L., & Weill, G. (1981). The SPOT satellite remote sensing mission. *Photogrammetric Engineering and Remote Sensing*, 47, 1163–1171.
- Dharmawan, I. W. S., & Siregar, C. A. (2008). Karbon tanah dan pendugaan karbon tegakan *Avicennia marina* (Forsk.) Vierh. di Ciasem, Purwakarta. *Jurnal Penelitian Hutan Dan Konservasi Alam*, 5(4), 317–328. <https://doi.org/10.20886/jphka.2008.5.4.317-328>.
- Dial, G., Bowen, H., Gerlach, F., Grodecki, J., & Oleszczuk, R. (2003). IKONOS satellite, imagery, and products. *Remote sensing of Environment*, 88(1-2), 23–36.
- Donato, D. C., Kauffman, J. B., Murdiyarso, D., Kurnianto, S., Stidham, M., & Kanninen, M. (2011). Mangroves among the most carbon-rich forests in the tropics. *Nature Geoscience*, 4(5), 293–297. <https://doi.org/10.1038/ngeo1123>
- FSI. (1996). *Volume equations for forests of India, Nepal and Bhutan*. Ministry of Environment and Forests, Government of India.
- Gibbs, H. K., Brown, S., Niles, J. O., & Foley, J. A. (2007). Monitoring and estimating tropical forest carbon stocks: Making REDD a reality. *Environmental Research Letters*, 2(4), 045023. <https://doi.org/10.1088/1748-9326/2/4/045023>
- Gnanamoorthy, P., Song, Q., Zhao, J., Zhang, Y., Liu, Y., Zhou, W., Sha, L., Fan, Z., & Deb Burman, P. K. (2021). Altered albedo dominates the radiative forcing changes in a subtropical forest

- following an extreme snow event. *Global Change Biology*, 27(23), 6192–6205. <https://doi.org/10.1111/gcb.15885>.
- Gnanappazham, L. (2020). Report on the project on Monitoring the health of Mangroves of Maharashtra state using Near real time satellite remote sensing data for period 2019–2020, IIST, doc No. IIST/MC\AnnRt\2019–20. <https://doi.org/10.1016/j.seares.2021.102162>.
- Google Earth. (2022). Satellite Imagery of Palghar, Mumbai, Thane, Raigarh, Ratnagiri, Sindhudurg, India. Google Earth. <https://www.google.com/earth/>.
- Gorelick, N., Hancher, M., Dixon, M., Ilyushchenko, S., Thau, D., & Moore, R. (2017). Google Earth Engine: Planetary-scale geospatial analysis for everyone. *Remote Sensing of Environment*, 202, 18–27. <https://doi.org/10.1016/j.rse.2017.06.031>
- Goward, S., Arvidson, T., Williams, D., Faundeen, J., Irons, J., & Franks, S. (2006). Historical record of Landsat global coverage. *Photogrammetric Engineering & Remote Sensing*, 72(10), 1155–1169. <https://doi.org/10.14358/PERS.72.10.1155>.
- Gunasekaran, P., Kankara, R. S., & Selvan, S. C. (2022). Mapping shoreline changes of the pocket beaches using Remote Sensing and GIS—A study in the north Konkan sector, west coast of India. *Journal of Earth System Science*, 131(4), 209. <https://doi.org/10.1007/s12040-022-01945-7>
- Harishma, K. M., Sandeep, S., & Sreekumar, V. B. (2020). Biomass and carbon stocks in mangrove ecosystems of Kerala, southwest coast of India. *Ecological Processes*, 9(1), 1–9. <https://doi.org/10.1186/s13717-020-00227-8>.
- Harris, N. L., Gibbs, D. A., Baccini, A., Birdsey, R. A., De Bruin, S., Farina, M., Fatoyinbo, L., Hansen, M. C., Herold, M., Houghton, R. A., & Potapov, P. V. (2021). Global maps of twenty-first century forest carbon fluxes. *Nature Climate Change*, 11(3), 234–240. <https://doi.org/10.1038/s41558-020-00976-6>.
- <https://earthexplorer.usgs.gov>
- Justice, C. O., Townshend, J. R. G., Vermote, E. F., Masuoka, E., Wolfe, R. E., Saleous, N., & Morisette, J. T. (2002). An overview of MODIS Land data processing and product status. *Remote sensing of Environment*, 83(1–2), 3–15.
- Kale, M. P., Chavan, M. E., & Lele, N. V. (2015). Restoration prioritisation at landscape level considering biodiversity, Carbon and Community Criteria with Special Reference to CDM/REDD+ - A Geomatics Perspective.
- Kale, M. P., Ravan, S. A., Roy, P. S., & Singh, S. (2009). Patterns of carbon sequestration in forests of Western Ghats and study of applicability of remote sensing in generating carbon credits through afforestation/reforestation. *Journal of the Indian Society of Remote Sensing*, 37, 457–471. <https://doi.org/10.1007/s12524-009-0035-5>.
- Kauffman, J. B., Heider, C., Cole, T. G., Dwire, K. A., & Donato, D. C. (2011). Ecosystem carbon stocks of Micronesian mangrove forests. *Wetlands*, 31, 343–352. <https://doi.org/10.1007/s13157-011-0148-9>.
- Komiyama, A., Pongpan, S., & Kato, S. (2005). Common allometric equations for estimating the tree weight of mangroves. *Journal of Tropical Ecology*, 21(4), 471–477. <https://doi.org/10.1017/S0266467405002476>.
- Kumar, T., Panigrahy, S., Kumer, P., & Parihar, J. S. (2013). Classification of floristic composition of mangrove forests using hyperspectral data: Case study of Bhitarkanika National Park, India. *Journal of Coastal Conservation*, 17, 121–132. <https://doi.org/10.1007/s11852-012-0223-2>.
- Lele, N., Kripa, M. K., Panda, M., et al. (2021). Seasonal variation in photosynthetic rates and satellite-based GPP estimation over mangrove forest. *Environmental Monitoring and Assessment*, 193, 61. <https://doi.org/10.1007/s10661-021-08846-0>
- Li, X., Li, X. B., Chen, Y. H., & Ying, G. (2007). Temporal responses vegetation to climate variables in temperate steppe of northern China *Chinese Journal of Plant Ecology*, 31(6), 1054. <https://doi.org/10.17521/cjpe.2007.0133>
- Ma, S., He, F., Tian, D., Zou, D., Yan, Z., Yang, Y., Zhou, T., Huang, K., Shen, H., & Fang, J. (2018). Variations and determinants of carbon content in plants: A global synthesis. *Biogeosciences*, 15(3), 693–702. <https://doi.org/10.5194/bg-15-693-2018>.
- Mandal, R., & Bar, R. (2018). *Mangroves for Building Resilience to Climate Change*. Apple Academic Press.
- Matsui, N., Suekuni, J., Nogami, M., Havanond, S., & Salikul, P. (2010). Mangrove rehabilitation dynamics and soil organic carbon changes as a result of full hydraulic restoration and re-grading of a previously intensively managed shrimp pond. *Wetlands Ecology and Management*, 18, 233–242. <https://doi.org/10.1007/s11273-009-9162-6>.
- Meiyappan, P., Roy, P. S., Sharma, Y., Ramachandran, R. M., Joshi, P. K., DeFries, R. S., & Jain, A. K. (2017). Dynamics and determinants of land change in India: Integrating satellite data with village socioeconomics. *Regional Environmental Change*, 17, 753–766. <https://doi.org/10.1007/s10113-016-1068-2>
- Mendiratta, P. & Gedam, S., (2015). Observing morphological changes in natural land form through archived satellite images: Case study of the Thane Creek. In *2015 International Conference on Technologies for Sustainable Development (ICTSD)* (pp. 1–6). IEEE. <https://doi.org/10.1109/ICTSD.2015.7095871>
- Nagler, T., Rott, H., Hetzenecker, M., Wuite, J., & Potin, P. (2015). The Sentinel-1 mission: New opportunities for ice sheet observations. *Remote Sensing*, 7(7), 9371–9389. <https://doi.org/10.3390/rs70709371>
- Nam, V. N. (2009). Personal Communication, in preliminary assessment of biomass and carbon content of mangroves in Solomon Islands, Vanuatu, Fiji, Tonga and Samoa. Duke N. (James Cook University: Center for Tropical Water & Aquatic Ecosystem Research)
- Nguyen, H. H., & Nguyen, T. T. H. (2021). Above-ground biomass estimation models of mangrove forests based on remote sensing and field-surveyed data: Implications for C-PFES implementation in Quang Ninh Province, Vietnam. *Regional Studies in Marine Science*, 48, 101985. <https://doi.org/10.1016/j.rsma.2021.101985>.
- Nguyen, L. D., Nguyen, C. T., Le, H. S., & Tran, B. Q. (2019). Mangrove mapping and above-ground biomass change detection using satellite images in coastal areas of Thai Binh Province, Vietnam. *Forest and Society*, 3(2), 248–261. <https://doi.org/10.24259/fs.v3i2.7326>
- Nyanga, C. (2020). The role of mangroves forests in decarbonizing the atmosphere. *Carbon-Based Material for Environmental Protection and Remediation*. <https://doi.org/10.5772/intechopen.92249>
- Opelele, O. M., Yu, Y., Fan, W., Chen, C., & Kachaka, S. K. (2021). Biomass estimation based on multilinear regression and machine learning algorithms in the Mayombe tropical forest, in the democratic republic of Congo. *Applied Ecology and Environmental Research*, 19, 359–377. https://doi.org/10.15666/aeer/1901_359377.
- Pambudi, G. P. (2011). Pendugaan biomassa beberapa kelas umur tanaman jenis *Rhizophora apiculata* Bl. pada areal PT. Bina Ovivi-pari Semesta Kabupaten Kubu Raya, Kalimantan Barat. [Skripsi]. Bogor (ID): Departemen Konservasi Sumberdaya Hutan dan Ekowisata, Fakultas Kehutanan Institut Pertanian Bogor. <http://repository.ipb.ac.id/handle/123456789/47632>.
- Pandya, M. R., Pathak, V. N., Shah, D. B., & Singh, R. P. (2014). Retrieval of surface reflectance using SACRS2: A scheme for atmospheric correction of ResourceSat-2 AWiFS data. *The International Archives of the Photogrammetry, Remote Sensing*

- and Spatial Information Sciences, XL–8, 865–868. <https://doi.org/10.5194/isprsarchives-XL-8-865-2014>.
- Petersson, H., Holm, S., Stahl, G., Alger, D., Fridman, J., Lehtonen, A., Lundström, A., & Makipaa, R. (2012). Individual tree biomass equations or biomass expansion factors for assessment of carbon stock changes in living biomass—A comparative study. *Forest Ecology and Management*, 270, 78–84. <https://doi.org/10.1016/j.foreco.2012.01.004>.
- Poli, D., Wolff, K., & Gruen, A. (2009). Evaluation of Worldview-1 stereo scenes. *International Archives of the Photogrammetry, Remote Sensing and Spatial Information Sciences*, 38(1), 202.
- Ragavan, P., Kumar, S., Kathiresan, K., Mohan, P. M., Jayaraj, R. S. C., Ravichandran, K., & Rana, T. S. (2021). Biomass and vegetation carbon stock in mangrove forests of the Andaman Islands, India. *Hydrobiologia*, 848, 4673–4693. <https://doi.org/10.1007/s10750-021-04651-5>.
- Rani, V., Nandan, S. B., Jayachandran, P. R., Preethy, C. M., Sreelekshmi, S., Joseph, P., & Asha, C. V. (2023). Carbon stock in biomass pool of fragmented mangrove habitats of Kochi, Southern India. *Environmental Science and Pollution Research*, 30, 1–17. <https://doi.org/10.1007/s11356-023-29069-5>
- Rout, L., Bhateja, Y., Garg, A., Mishra, I., Moorthi, S. M. & Dhar, D. (2019). DeepSWIR: A deep learning based approach for the synthesis of short-wave InfraRed Band using multi-sensor concurrent datasets. <https://doi.org/10.48550/arXiv.1905.02749>
- Roy, P.S., Roy, A., Joshi, P. K., Kale, M.P., Srivastava, V.K., Srivastava, S.K., Dwevidi, R.S., Joshi, C., Behera, M.D., Meiyappan, P., Sharma, Y., Jain, A.K., Singh, J.S., Palchowdhuri, Y., Ramachandran, R.M., Pinjarla, B., Chakravarthi, V., Babu, N., Gowsalya, M.S., Thiruvengadam, P., Kotteeswaran, M., Priya, V., Yelishetty, K.M.V.N., Maithani, S., Talukdar, G., Mondal, I., Rajan, K.S., Narendra, P.S., Biswal, S., Chakraborty, A., Padalia, H., Chavan, M., Pardeshi, S.N., Chaudhari, S.A., Anand, A., Vyas, A., Reddy, M.K., Ramalingam, M., Manonmani, R., Behera, P., Das, P., Tripathi, P., Matin, S., Khan, M.L., Tripathi, O.P., Deka, J., Kumar, P., & Kushwaha, D. (2016). Decadal land use and land cover classifications across India, 1985, 1995, 2005. *Remote sensing*, 7(3), 2401–2430. <https://doi.org/10.3390/rs70302401>.
- Saxena, A., Jha, M. N., & Rawat, J. K. (2003). Forests as carbon sink – The Indian scenario. *Indian Forester*, 129(7), 807–814.
- Singh, B., Verma, A. K., Tiwari, K., & Joshi, R. (2023). Above ground tree biomass modeling using machine learning algorithms in western Terai Sal Forest of Nepal. *Heliyon*, 9(11), e21485. <https://doi.org/10.1016/j.heliyon.2023.e21485>
- Sun, H., Qie, G., Wang, G., Tan, Y., Li, J., Peng, Y., Ma, Z., & Luo, C. (2015). Increasing the accuracy of mapping urban forest carbon density by combining spatial modeling and spectral unmixing analysis. *Remote Sensing*, 7(11), 15114–15139. <https://doi.org/10.3390/rs71115114>.
- Tiwari, A. K. (1992). Component-wise biomass models for trees. A nonharvest technique. *Indian For*, 118, 405–410.
- Toutin, T., & Cheng, P. (2002). QuickBird—a milestone for high resolution mapping. *Earth Observation Magazine*, 11(4), 14–18.
- Trumper, K. (2009). The natural fix?: the role of ecosystems in climate mitigation: a UNEP rapid response assessment. UNEP/Earthprint.
- Wang, G., Guan, D., Zhang, Q., Peart, M. R., Chen, Y., & Peng, Y. (2015). Distribution of dissolved organic carbon and KMnO₄-oxidizable carbon along the low-to-high intertidal gradient in a mangrove forest. *Journal of Soils and Sediments*, 15, 2199–2209. <https://doi.org/10.1007/s11368-015-1150-2>.
- Wang, L., Jia, M., Yin, D., & Tian, J. (2019). A review of remote sensing for mangrove forests: 1956–2018. *Remote Sensing of Environment*, 231, 111223. <https://doi.org/10.1016/j.rse.2019.111223>.
- Xia, Q., Qin, C. Z., Li, H., Huang, C., & Su, F. Z. (2018). Mapping mangrove forests based on multi-tidal high-resolution satellite imagery. *Remote Sensing*, 10(9), 1343. <https://doi.org/10.3390/rs10091343>
- Zanne, A. E., Lopez-Gonzalez, G., Coomes, D. A., Ilic, J., Jansen, S., Lewis, S. L., & Chave, J. (2009). Global wood density database. Dryad Digital Repository. <https://doi.org/10.5061/dryad.235>.
- Zhao, X., Ma, X., Chen, B., Shang, Y., & Song, M. (2022). Challenges toward carbon neutrality in China: Strategies and countermeasures. *Resources, Conservation and Recycling*, 176, 105959. <https://doi.org/10.1016/j.resconrec.2021.105959>.
- Zhu, B., Feng, T., Gong, D., Jiang, S., Zhao, L., & Cui, N. (2020). Hybrid particle swarm optimization with extreme learning machine for daily reference evapotranspiration prediction from limited climatic data. *Computers and Electronics in Agriculture*, 173, 105430. <https://doi.org/10.1016/j.compag.2020.105430>

Publisher's Note Springer Nature remains neutral with regard to jurisdictional claims in published maps and institutional affiliations.

Springer Nature or its licensor (e.g. a society or other partner) holds exclusive rights to this article under a publishing agreement with the author(s) or other rightsholder(s); author self-archiving of the accepted manuscript version of this article is solely governed by the terms of such publishing agreement and applicable law.